Four residues of the extracellular N-terminal domain of the NR2A subunit control high-affinity Zn2+ binding to NMDA receptors.

A. Fayyazuddin, A. Villarroel, A. Le Goff, J. Lerma, J. Neyton

Four residues of the extracellular N-terminal domain of the NR2A subunit control high-affinity Zn binding to NMDA receptors

Amir Fayyazuddin[1], Alvaro Villarroel[2], Anne Le Goff[1], Juan Lerma[2] and Jacques Neyton[1]

[1] Laboratoire de Neurobiologie
Ecole Normale Supérieure
CNRS UMR 8544
46 rue d'Ulm
75005 Paris
France

and

[2]Instituto Cajal
Consejo Superior de Investigaciones Cientificas
28002 Madrid
Spain

Running title: High affinity Zn binding site in NMDA receptors

Key words: glutamate receptor, zinc, LIVBP, inhibition

Corresponding author: Dr. Jacques Neyton
Laboratoire de Neurobiologie, Ecole Normale Supérieure
46, rue d'Ulm, 75005 Paris - France

Tel: 33 1 44 32 38 94

Fax: 33 1 44 32 38 87

Email: neyton@biologie.ens.fr

SUMMARY

NMDA receptors are allosterically inhibited by Zn^{2+} ions in a voltage-independent manner. The apparent affinity for Zn of the heteromeric NMDA receptors is determined by the subtype of NR2 subunit expressed with NR2A-containing receptors being the most sensitive (IC_{50} ~ 20 nM) and NR2C-containing receptors being the least sensitive (IC_{50} ~ 30 μM). Using chimeras constructed from these two NR2 subtypes, we show that the N-terminal LIVBP-like domain of the NR2A subunit controls the high-affinity Zn inhibition. Mutations at four residues in this domain markedly reduce Zn affinity (by up to >500-fold) without affecting either receptor activation by glutamate and glycine or inhibition by extracellular protons and Ni^{2+} ions indicating that these residues most likely participate in high-affinity Zn binding.

INTRODUCTION

Channel gating, along with ionic selectivity, constitutes one of the two fundamental properties that define the physiological role of an ion channel. It is therefore not surprising that the gating properties of ion channels are often the target of allosteric modulators. NMDA receptors, members of the ionotropic glutamate receptor family that have been implicated in neuronal development and synaptic plasticity as well as pathological disorders, constitute a typical example of heavily modulated channels. Their activation requires the presence of two co-agonists, glutamate and glycine, and their gating is affected by several extracellular agents including protons, several divalent cations and polyamines which act non-competitively with respect to the agonists (reviewed in McBain and Mayer, 1994; Dingledine et al., 1999). For each of these modulators there must exist a binding site and transduction machinery linking the binding site to the "gate". However, the molecular structures underlying the binding of these modulators, their link with the gating mechanism, as well as the gating mechanism itself, remain poorly understood. We have begun to look at the structural determinants of one such modulation, the voltage-independent inhibition by extracellular Zn^{2+} ions and have identified several residues that are closely related to Zn binding, the first step in the Zn inhibition mechanism.

NMDA receptors are heteromers consisting of two different subunits, NR1 and NR2 that share a common membrane topology with all other ionotropic glutamate receptor subunits. Each subunit contains three transmembrane segments (TM1, TM3 and TM4), a P-loop region (called TM2 according to the originally proposed topology) and a cytoplasmic C-terminus (see Dingledine et al., 1999). The extracellular domains are made by the large N-terminal region (~550 aa) preceding TM1 and by a smaller loop (~150 aa) between TM3 and TM4. A first part of the N-terminus (the first 380 amino acids) has a weak sequence similarity with a bacterial periplasmic protein called LIVBP (for Leucine, Isoleucine, Valine Binding Protein; O'Hara et al., 1993; Masuko et al., 1999). The rest of the N-terminal along with a portion of the loop between TM3 and TM4 shows sequence similarity to other bacterial amino acid binding proteins such as QBP (for glutamine binding protein) and LAOBP (Lysine, Arginine, Ornithine Binding Protein; Nakanishi et al., 1990; O'Hara et al.,

1993; Stern-Bach et al., 1994). This second extracellular domain has been shown to make up the agonist binding site with specificity for glycine in the NR1 subunits and for glutamate in the NR2 subunits (see Dingledine et al., 1999).

Extracellular Zn induces two types of inhibitory effects on NMDA receptors, a voltage-dependent channel block much like the one produced by Mg^{2+} ions, and a voltage-independent inhibition - hereon referred to as "inhibition" - due to a decrease in the open probability of the receptor channel (Christine and Choi, 1990; Legendre and Westbrook, 1990). Previous studies on recombinant receptors showed that voltage-independent Zn inhibition is primarily determined by the type of NR2 subunit present (Williams, 1996; Chen et al., 1997; Paoletti et al., 1997; Traynelis et al., 1998). Receptors containing NR2A subunits have a high sensitivity to Zn (IC_{50} ~ 20 nM) and the inhibition is partial, allowing ~ 20% of the channels to remain active at saturating Zn concentrations, whereas the receptors containing other NR2 subunits (2B, 2C or 2D) have a lower sensitivity to Zn (IC_{50} ranging between 0.5 μM for NR2B and 30 μM for NR2C) and the inhibition is complete at high concentrations of Zn. As a consequence of their high Zn sensitivity, NR2A-containing receptors are expected to be tonically inhibited by the low levels of Zn (usually above 50 nM) found as contaminants in standard solutions in most laboratories. Indeed, application of heavy metal chelators potentiates NR1-NR2A receptors, presumably by removing the contaminating Zn (Paoletti et al., 1997).

In characterizing the mechanism of Zn inhibition, an important step is to locate precisely where the inhibiting Zn^{2+} ions bind on the NMDA receptor. In this study we concentrated on the high affinity Zn binding site found specifically in NR2A-containing receptors. Given that this inhibition by Zn showed no sensitivity to voltage, our starting hypothesis was that the high affinity Zn inhibitory site should be located in the extracellular domains of the NR2A subunit. We began by roughly locating this site within the NR2A extracellular domains using receptors containing chimeric NR2 subunits made from NR2A and NR2C, coexpressed with NR1 in *Xenopus* oocytes. Measurements, under two electrode voltage clamp, of the Zn inhibition in various chimeras allowed the identification of an N-terminal region of about 380 amino acids, as being necessary for high affinity Zn binding. Interestingly, this region coincides with the LIVBP-like region. Next, using a point mutation strategy, we identified four residues in this N-terminal domain that may represent, at least in part, the molecular determinants of the high affinity Zn binding site. Mutations at these

residues markedly decrease (> 50 fold) the apparent affinity for Zn of NR2A-containing receptors, and they specifically target the high affinity Zn inhibition: neither the apparent affinities for either agonist, nor other types of gating modulation such as those by protons or nickel are affected. While this work was in progress, another study proposed that two residues in the N-terminal of the NR2A subunit (including one of the residues discussed in this report) may constitute part of the Zn binding site (Choi and Lipton, 1999).

RESULTS

A major molecular determinant of the high-affinity voltage-independent Zn inhibition resides in the N-terminal LIVBP-like domain of the NR2A subunit.

Given the subunit specificity and voltage-independence of the Zn inhibition, we restricted our search for the high affinity Zn binding site to the extracellular region of the NR2A subunit. In order to locate which part of this large region (> 500 aa) is most likely to contain the high affinity Zn binding site, we measured Zn sensitivity of receptors consisting of NR1 subunits coexpressed with chimeric subunits made by swapping different regions between the most sensitive subunit, NR2A, and the least sensitive one, NR2C. Fig.1 compares Zn inhibition observed with wild type NR2A or NR2C subunits with that observed with chimeras in which the region N-terminal to TM1 from one subunit has been replaced by the homologous region from the other subtype. At a steady voltage of -60 mV, an application of 50 nM buffered Zn (see Experimental Procedures), a concentration too low to produce a voltage-dependent block of NMDA receptors (Paoletti et al., 1997), induces a strong inhibition (~ 62%) of the response evoked by saturating doses of glutamate and glycine (100 μM each) in wild-type NR2A-containing receptors (Fig.1A1). By contrast, wild-type NR2C-containing receptors are barely inhibited at this concentration (Fig.1A2). The Zn sensitivity of the receptors containing chimeric subunits depends on the donor of the pre-TM1 N-terminal region. Thus receptors containing chimeras with the N-terminal of NR2C [NR2C/A(564), Fig.1A3] are only slightly, if at all, inhibited by 50 nM Zn whereas receptors containing chimeras with the N-terminal of NR2A [NR2A/C(553), Fig.1A4] are strongly inhibited (~ 55%).

Full Zn dose-inhibition curves (Fig.1B) were obtained for these four NR2 constructs in a series of experiments performed with -100/+50 mV voltage ramps (see Experimental Procedures). The current was measured at +50 mV to avoid contamination of the voltage-independent inhibition by the voltage-dependent Zn block in the 1 μM - 1 mM concentration range. Experimental data were fitted by a Michaelis inhibition function (see Experimental Procedures). The curve obtained with NR2A/C(553) chimera containing receptors resembles that of receptors containing NR2Awt subunits in that the IC_{50} for both receptors is in the 10 - 100 nM range [67 nM for NR2A/C(553) and 14 nM for NR2Awt] and they saturate at 75% maximum inhibition. On the other hand, receptors containing

the chimera NR2C/A(564) are similar to NR2Cwt in IC_{50} values [6.7 μM for NR2C/A(564) versus 23 μM for NR2C] as well as maximal inhibition (close to 100% in both cases). These results show that high affinity Zn inhibition requires the presence of the region preceding TM1 from NR2A.

Next, using a set of NR2A/NR2C chimeras (see Experimental Procedures for a precise definition of the chimeras), we attempted to localize the high-affinity Zn binding site to a smaller region of the NR2A N-terminal. Briefly, the N-terminal region of NR2 subunits was subdivided into six regions numbered N1-N6 and each of these regions was replaced in NR2A by the homologous fragment of NR2C. All of these constructs, except NR2A'(CN1), resulted in functional NR2 subunits as indicated by the amplitude of the glutamate responses recorded in oocytes (see Experimental Procedures). To study the potential implication of the N1 region in the high-affinity Zn binding site, this region was split into two smaller fragments (N1a and N1b) which were deleted one at a time in NR2A, instead of being replaced by the homologous NR2C fragments, leading to the functional constructs NR2A'(ΔN1a) and NR2A'(ΔN1b) respectively. Zn inhibition was measured at +50 mV for each of the chimeric constructs and the IC_{50} values were obtained from the dose-inhibition curves. The results from these experiments are plotted in Fig.2. The top 4 rows plot the results obtained with the constructs of Fig.1. Data from chimeras in which one of the segments N1-N6 had been replaced by the homologous region of NR2C or deleted altogether are shown in rows 6-12 and NR2A', the parental NR2A from which each of these chimeras was constructed is shown in row 5. NR2A' had an IC_{50} of 29 nM which is very close to the IC_{50} of NR2Awt. In contrast, chimeras involving N1, N2 and N3 regions all present a markedly increased (more than 50 fold) Zn IC_{50}. The Zn IC_{50}s of chimeras involving regions more proximal to TM1 are either only moderately increased (by 10 fold in the case of N6), not significantly affected (N5), or even decreased (by 55 fold in the case of N4).

Taken together these results suggest that the high affinity Zn binding site may be located in the N1-N3 regions. This idea is supported by the observation that the subunit NR2C(AN1-4), formed by replacement of segments N1-N4 in NR2C by the homologous region of NR2A, is highly sensitive to Zn (Fig.2, row 13). Interestingly, the region consisting of the segments N1-N3 has been shown to share sequence similarity with one type of bacterial periplasmic protein, the Leucine-Isoleucine-Valine-Binding-Protein (LIVBP) (O'Hara et al., 1993; Masuko et al., 1999). We will hereon call this region the LIVBP-like domain.

While the exchange of the N2 or N3 regions reduced the apparent affinity for Zn by at least 50 fold, the Zn inhibition was not abolished and the resulting receptors were still sensitive to micromolar concentrations of Zn. One possibility is that the LIVBP-like domains in NR2A and NR2C contain amino acid residues that contribute to a high affinity Zn binding site in NR2A and a low affinity site in NR2C so that replacement of fragments in NR2A with homologous fragments of NR2C switches the sensitivity of the resulting receptor to an NR2C-like sensitivity. A strong argument against this possibility is that receptors containing the construct NR2A'(ΔN1-3)tr (Fig.2, row 14) in which the full LIVBP-like domain has been deleted still retain a Zn IC_{50} in the low micromolar range. We were particularly worried that such a large deletion in an NR2 subunit will produce a non functional subunit and that the phenotype observed with this deletion construct might correspond to that of "homomeric" NR1 receptors (see Experimental Procedures). However coinjection into oocytes of NR1 with NR2A'(ΔN1-3)tr leads to large glutamate responses (> 1μA at -60 mV, similar to those recorded with wild type NR2A) indicating that this NR2 construct is functional.

Identification of individual residues important for high affinity Zn inhibition

The results from chimeric receptors described above suggested the presence of major determinants of the high affinity Zn binding site within the extracellular LIVBP-like domain in the N-terminal of NR2A. Our next strategy was to use point mutations to try to identify individual amino acid residues that may be important for high affinity Zn inhibition. In most proteins, heavy metal ions are usually coordinated by nitrogen, sulfur, or oxygen atoms found in side chains of histidine, cysteine, aspartate and glutamate residues (Glusker, 1991) making these residues logical targets for mutagenesis. Based on an analysis of published NR2 sequence alignments (Ishii et al., 1993), a first series of mutations were made at positions that were occupied by a putative Zn ligand. (i.e. H, C, D or E) in NR2A, but that were not conserved (even in a broad degenerate way, i.e. as polar or charged) in the homologous NR2C position (Fig.3, triangles). We also considered the possibility that the high affinity Zn binding site may contain residues that are conserved between NR2A and NR2C but, because of differences in the local environment, may not serve this function in NR2C, or, because of the absence of other partners, may not be sufficient to make a high affinity binding site in

NR2C. Therefore, a second series of mutations was carried out to replace some conserved C, D and E residues (Fig.3, diamonds). In this series, we also mutated some positively charged residues (K and R) which, in addition to a possible (but difficult to test) influence on the Zn binding site 3D structure, may also exert electrostatic repulsion on the Zn^{2+} cation.

Mutants were screened by measuring the level of inhibition at two Zn concentrations: 50 nM, a concentration 3 fold higher than the IC_{50} of NR2Awt-containing receptors and 500 nM, a saturating concentration for these receptors (Table I). We arbitrarily considered as "strongly" affected those mutants that had relative current amplitudes that were larger by more than 2-fold from the relative currents of wild type receptors (bold and boxed or underligned in Fig.3 and Table I, respectively). "Moderately" affected mutants were defined as those that had relative currents larger or smaller than wild type by more than 1.25-fold and less than 2-fold (simply bold in Fig.3 and Table I). Of the 45 positions mutated, which all gave functional receptors, our screening strategy detected 11 mutations (H42A, H44A, D78A, H128S, D207A, E211Q, K233R, R244G, E266S, H358A and K374S) resulting in a significant modification of the Zn inhibition with four mutants, H44A, H128S, K233R and E266S, that could be classified as "strongly" affected. Complete Zn inhibition curves were constructed for these 11 mutants (see Fig.4 for H44A, H128S, K233R and E266S) and the parameters of the fits performed with equation 1 (see Experimental Procedures) are given in Table II. The results from the inhibition curves confirm our empirical quantification: the mutations H42A, D78A, D207A, E211Q, H358A and K374S moderately increase the Zn IC_{50} by 2 to 25 fold while the R244G mutation results in a 35 fold *decrease* in Zn IC_{50}. The mutations H44A, H128S, K233R and E266S have a more drastic effect on the Zn inhibition: H44A decreases the apparent Zn affinity by 70 fold, H128S by 520 fold, K233R by 200 fold and E266S by 425 fold, respectively.

Controlling for Zn-binding specificity of the mutations affecting Zn inhibition

Our mutagenesis scan resulted in the identification of 4 residues, H44, H128, K233 and E266, whose mutation profoundly affects the apparent affinity of the inhibitory Zn binding site. The nature of these residues (except for the lysine, but see discussion), as well as the amplitude of the mutation-induced shifts in Zn IC_{50} (between 70 and 500 fold) support the idea that they may directly participate in the high affinity Zn binding site. However, a strong effect of a mutation on the IC_{50} is not a proof that the residue participates in the binding process. Indeed, mutations that affect the

gating equilibrium (hereon called "remote"to distinguish from mutations which directly affect Zn binding) may reciprocally affect the ligand binding equilibrium (Colquhoun, 1998). Quantitatively, the effects of such "remote" mutations can be large.

Two mutations in the P-loop region (TM2) of the NR1 subunit, W590C and N598C, constitute typical examples of such "remote" mutations with regard to the high-affinity Zn binding site. NR1-W590 has been located in the inner vestibule of the channel (Kuner et al., 1996) and NR1-N598 is part of the selectivity filter, deep in the pore, where blocking Mg^{2+} ions bind (see Dingledine et al., 1999). The locations of these residues make it very improbable that they participate in the high-affinity Zn inhibitory site, which, given the lack of voltage-dependence of the Zn inhibition, must be outside the transmembrane field. Indeed, the mutation NR2A-N595K, which introduces a positive charge in the selectivity filter (i.e. in the close vicinity of NR1-N598), fully prevents access to the pore for divalent cations, but leaves unaffected the high-affinity Zn inhibition (see Paoletti et al., 1997). Despite their probable distance from the Zn binding site, the mutants NR1-W590C and NR1-N598C, coexpressed with NR2Awt both strongly decrease Zn inhibition. The amplitudes of the relative current measured at -60 mV in the presence of 0.5 μM Zn in the bath (0.92 ± 0.04, $n = 4$ and 0.85 ± 0.05, $n = 3$, respectively) are comparable to that of the "strong" mutants (see Table I). In fact, mutations at position NR1-N598 have already been shown to have pleitropic effects on gating (Schneggenburger and Ascher, 1997), spermine potentiation and proton inhibition (Kashiwagi et al., 1997; Traynelis et al., 1998; Zheng et al., 1999) and Zn inhibition (Traynelis et al., 1998).

How can one distinguish a mutation in the Zn binding site from a "remote" one? "Remote" mutations should non-specifically affect the binding of other ligands acting on gating, whereas a mutation of the Zn binding site has a much higher probability of specifically affecting Zn inhibition (except, of course, if the mutated residue also participates in the gating mechanism). In order to test the specificity for Zn inhibition of the four "strong" mutations and of several "moderate" mutations that had been identified, we compared the effects of these mutations with those of two "remote" mutations (NR1-W590C and NR1-N598C) on several gating modulations of NMDA receptors: i) the activation by the two agonists glutamate and glycine; ii) the inhibition by extracellular protons; and iii) the voltage-independent inhibition by extracellular Ni^{2+} ions.

Dose-response curves for glutamate and glycine were obtained under Zn-free conditions for receptors containing NR1wt and NR2Awt subunits, receptors containing NR1wt and one of the

NR2A mutants H44A, H128S, K233R, R244G and E266S, and receptors containing either NR1-W590C or NR1-N598C and NR2Awt. Table III shows the parameters of equation 3 used to fit the curves (see Experimental Procedures). A comparison with wild type shows no significant variation in the fitting parameters of the five NR2A mutants. In contrast the two "remote" NR1 mutants have a 10-fold greater affinity for both glycine and glutamate relative to wild-type.

Extracellular protons in the physiological concentration range (around pH 7) have been shown to inhibit NMDA receptors via a decrease in their open probability (Traynelis and Cull-Candy, 1990). Residues from different parts of the extracellular domains of NR1 subunits appear to be involved in this modulation (see Dingledine et al., 1999). Proton inhibition curves obtained from receptors containing each of the "strong" NR2A mutants (H44A, H128S, K233R and E266S) were not much different, if at all, from those of wild type receptors (Fig. 5A). In contrast, NR1-W590C and NR1-N598C mutations induced a significant increase in proton IC_{50} (7 and 4 fold, respectively, Fig. 5A). Three of the tested "moderate" NR2A mutants (H42A, D207A and K374S) showed proton inhibition curves that were indistinguishable from that of wild type receptors (not shown). However, the mutation NR2A-R244G induced a 2 fold decrease in proton IC_{50} (Fig. 5A).

Extracellular Ni^{2+} ions, in addition to inducing a voltage-dependent block very similar to that of Mg, also inhibit in a voltage-independent manner several recombinant NMDA receptor subtypes (those containing NR2A, NR2B or NR2D subunits; Paoletti and Neyton, manuscript in preparation). As for protons, Ni inhibition curves of receptors containing the "strong" NR2A mutants did not significantly differ from that of wild type receptors [for NR2A-H44A and NR2A-H128S, only one concentration of nickel was tested (100 μM) and the relative currents were close to that of wild type receptors: 0.42 ± 0.03, $n = 3$ for H44A; 0.55 ± 0.04, $n = 3$ for H128S; 0.52 ± 0.06, $n = 5$ for wild type]. In contrast again, both NR1-W590C and NR1-N598C mutations induced a 5 fold increase in Ni IC_{50}. The "moderate" NR2A mutant R244G did not affect Ni sensitivity (with 100 μM Ni, the relative current was 0.55 ± 0.07, $n = 7$).

DISCUSSION

Previous studies (Williams, 1996; Chen et al., 1997; Paoletti et al., 1997; Traynelis et al., 1998) have shown that the voltage-independent inhibition of NMDA receptors by extracellular Zn depends on the subtype of the NR2 subunit present, with receptors containing NR2A subunits having a remarkably high apparent affinity for Zn (IC_{50} around 20 nM). This work aimed at identifying the molecular determinants of the high affinity Zn binding site. Given the voltage-independence and the subunit specificity of the Zn inhibition, we hypothesized that the high affinity Zn binding site should be located in an extracellular domain of the NR2A subunit, and indeed found that the presence of the LIVBP-like domain of NR2A is required and sufficient to confer high affinity Zn inhibition to receptors expressing chimeric NR2A/NR2C subunits. This, combined with the fact that deletion of this domain does not prevent expression of functional receptors (see Fig. 2), strengthens the proposal that the N-terminal region preceding the agonist binding domain constitutes a modular domain involved in gating modulation (Köhr et al., 1994; Krupp et al., 1998; Villarroel et al., 1998; Masuko et al., 1999). A point mutagenesis scan through the LIVBP-like domain of NR2A allowed us to identify several residues that, when mutated, severely affected high affinity Zn inhibition. The amplitude and specificity of the effects of individual point mutations on the Zn inhibition favor four residues, two histidines (H44 and H128), a lysine (K233) and a glutamate (E266) as being closely associated with the high affinity Zn inhibitory site. Another study, published while this work was in progress (Choi and Lipton, 1999), already proposed that one of these residues, NR2A-H44, together with NR2A-H42 constitute part of the high affinity Zn binding site. As discussed below (third section of Discussion), we agree on this proposal for NR2A-H44, but propose another interpretation for the role of NR2A-H42.

NR2A-containing NMDA receptors may possess two types of voltage-independent Zn inhibitory sites

Even though several mutations in the NR2A N-terminal were able to shift Zn affinity by several orders of magnitude, none of them were able to completely eliminate voltage-independent Zn inhibition. The four most effective mutations were only able to shift the Zn IC_{50} into the low μM

range, which is on the same order as the Zn affinity of non-NR2A containing recombinant receptors (around 1 μM for NR2B, see Williams, 1996; Chen et al., 1997; Paoletti et al., 1997; Traynelis et al., 1998; around 20 μM for NR2C, Paoletti et al., 1997; Traynelis et al., 1998; and around 2 μM for NR2D, Fayyazuddin and Neyton, unpublished results). One possible explanation for these observations is that there is a *single* inhibitory Zn binding site in each subtype of the NR2 subunit and these sites share conserved amino acids at homologous locations. In this case the residues specific to NR2A and (for example, H44) would be the ones that confer high affinity to the Zn binding site. The low affinity Zn binding site would be made up of residues partly conserved across NR2 subtypes (H128, K233 or E266, for example). Under this scheme, as recently proposed by Choi and Lipton (1999), the binding site could retain a basal level of affinity for Zn even if one of the important residues is mutated. If this were the case, mutating the non-conserved residue, H44, along with a conserved residue should produce additive effects on apparent Zn affinity. This is not the case as shown with the triple mutant NR2A-H42A-H44A-E266A (see table II), which has an IC_{50} very close to that of NR2A-H44A and NR2-E266A mutants. Moreover, receptors made with NR2A subunits lacking the entire LIVBP-like domain (NR2A'(ΔN1-3)tr, see Fig.2, last row) retain an affinity for Zn in the low μM range, not significantly different from the affinity of receptors containing the most effective mutations. A possibility remains that another domain, located elsewhere on the receptor, forms a low affinity site that is transformed into a high affinity site in the presence of the LIVBP-like domain. As we shall see in the next paragraph, this is unlikely.

Based on the two arguments presented above, we favor the following alternative explanation: i) all NMDA receptor types possess a low affinity Zn inhibitory site; ii) those containing NR2A have an additional high affinity site; and iii) in NR2A-containing receptors, Zn occupancy at both sites leads to partial inhibition through mechanisms that converge at some point. Under this hypothesis, the low affinity Zn binding site of NR2A would be normally masked by the high affinity site because the receptors could be already maximally inhibited at concentrations of Zn much lower than those needed to activate the low affinity site. However, when the high affinity Zn binding site is perturbed, either by one of the four "strong" NR2A mutations or by deletion of the NR2A LIVBP-like domain, the low affinity binding site is unmasked and in these constructs the Zn IC_{50} reflects that of the low affinity site. In addition to the strikingly similar shifts in Zn IC_{50} induced by each "strong" mutation and by the deletion construct, support for this interpretation is provided by the fact that the Zn

inhibition dose-response curve of NR1-N598C/NR2Awt receptors is biphasic at +50 mV (not shown), with a minor high-affinity component (IC_{50} ~ 20 nM) that saturates at 85% of the control current and a major low-affinity component (IC_{50} ~ 7 μM) that saturates at 20% of the control current. These results, showing the simultaneous presence of two different Zn binding sites in receptors containing wild type NR2A but mutated NR1 subunits, argue strongly for the potential presence in NR2A-containing receptors of two Zn binding sites with differing affinities for Zn. So far we have found no NR2A mutants inducing a Zn IC_{50} increase significantly larger than that observed with the N1-3 deletion mutant. Therefore, the sole indication regarding the localization of the potential low affinity Zn binding site is that it must be outside the NR2A LIVBP-like domain, whether in the extracellular domains of NR1 or in the agonist binding domain of NR2A.

Specificity of the effects of mutations on Zn inhibition and convergence of NMDA receptor modulations

Zn inhibits NMDA receptors by reducing the open probability of activated receptors (Christine and Choi, 1990; Legendre and Westbrook, 1990), i.e. voltage-independent binding of Zn on extracellular binding sites results in changes in some of the conformational equilibria involved in the gating mechanism. Microscopic reversibility in thermodynamic equilibria implies that if binding of Zn modifies certain gating equilibria, modifications of these gating equilibria should reversibly affect Zn binding, and therefore, a decrease in apparent affinity for Zn could result from modifications in the gating mechanism as well as from perturbations of the Zn binding site itself. However, whereas the first mechanism is expected to alter the effects of other agents acting on gating, the second should specifically affect Zn inhibition. The four NR2A "strong" mutations identified in this study (H44A, H128S, K233R and E266S) do not appear to affect the gating mechanism itself because in receptors containing these mutations, Ni inhibition or (in the absence of Zn) activation by glutamate and glycine (see Table III) and voltage-independent inhibition by extracellular protons (Fig.5) are similar to those recorded in wild type receptors. This indicates that, within the chain of events linking Zn binding to the decrease in open probability, these mutations must affect either the Zn binding reaction itself or a step very close to it. Many other mutations affect high affinity Zn inhibition and several of them are not located in the NR2A LIVBP-like domain. Interestingly, most of these

mutations were first identified as affecting gating modulators other than Zn [NR1-E342Q and NR1-D669N which decrease proton sensitivity (Kashiwagi et al., 1996; Traynelis et al., 1998; Williams et al., 1995); NR1-C744A and NR1-C798A which decrease sensitivity to reducing agents (Sullivan et al., 1994)]. This also appears to be the case for two other mutations described in this paper, NR1-W590C and NR1-N598C, which are both located in the putative pore loop of NR1. Both mutations have pleiotropic effects on Zn inhibition, glutamate and glycine activation (table III), as well as inhibition due to protons and Ni (Fig. 5). Strikingly, mutations of the homologous residues of the NR2A subunit (W587, N595 and N596) do not perturb the high-affinity Zn inhibition (Fayyazuddin and Neyton, unpublished results) suggesting that the involvement of pore residues in the gating mechanism is specific to NR1 subunits.

Within the NR2A LIVBP-like domain, several mutations having "moderate" effects on Zn inhibition were tested for Zn inhibition specificity. Some of these, which all reduce sensitivity to Zn, were found to be without effect on proton inhibition (H42A, D207A and E211Q, not shown). However, R244G, which induces a marked increase in Zn sensitivity (see Table I and II) also raised the sensitivity to protons (Fig.5A), but did not affect glutamate and glycine activation curves (Table III). The fact that mutations in the NR2A LIVBP-like domain can lead to either specific effects on Zn inhibition or pleiotropic effects on different gating modulations is not surprising. "Specific" residues could be participating in shaping the 3D structure around Zn-coordinating residues. "Pleiotropic" residues may affect gating modulation at a point distant from the Zn binding step itself, for example at the interface of the LIVBP-like domain and the remainder of the protein. In this regard, it is worth pointing out that the NR2A LIVBP-like domain was recently identified as one of the major determinants of Ca- and glycine-independent desensitization (Krupp et al., 1998; Villarroel et al., 1998). Zn binding itself is not required for desensitization because receptors desensitize even in the presence of Zn chelators (see for example Paoletti et al., 1997, Fig. 8). However, the kinetics of onset of desensitization are accelerated by Zn (Chen et al., 1997). Thus, Zn inhibition and desensitization may converge on a common step of the gating process with, for example, Zn binding leading to stabilization of a desensitized state. Analyzing the effects on desensitization of the NR2A mutants identified in this study may help to clarify this point.

Are H44, H128, K233 and E266 making the high affinity Zn binding site in the NR2A LIVBP-like extracellular domain?

Zn binding sites have been characterised in many metalloproteins in which the Zn ion participates in catalysis or helps to stabilize the three dimensional conformation of the peptide chain (Lippard and Berg, 1997). At these sites, Zn is tightly bound with an affinity in the picomolar to nanomolar range. X-ray diffraction studies have shown that Zn is usually coordinated in a tetrahedral, square planar or octahedral geometry by at least three amino acid ligands which often include a doublet of cysteines or histidines seperated by a short spacer (Christianson, 1991; Glusker, 1991; Vallee and Auld, 1993; Karlin and Zhu, 1997). Modulatory Zn binding sites, where Zn binds reversibly with lower affinities (10 nM to 10 μM), are present in several ligand-gated channels including members of the $GABA_A$ (Wooltorton et al., 1997; Horenstein and Akabas, 1998) glycine (Laube et al., 1995) and ATP (Li et al., 1997) families of ligand-gated channels and in most cases have not been well-characterized. A histidine residue located in the second transmembrane segment of $GABA_A$ subunits has been implicated in the voltage independent Zn inhibition of $GABA_A$ receptors (Wooltorton et al., 1997;Horenstein and Akabas, 1998). Two recent studies have implicated histidine residues in the sequence H-X-H as forming part of the Zn inhibitory binding site in glycine (Harvey et al., 1999) and NMDA receptors (Choi and Lipton, 1999; our work, however, is not in full agreement with this interpretation as discussed below).

In this paper, we show that several residues in the NR2A LIVBP-like domain are important for high affinity Zn inhibition and of these, four residues, H44, H128, K233 and E266, appear closely associated with the Zn binding site because of the large shift in Zn affinity and specificity for Zn inhibition of mutations at these residues. Given the nature of their side chains, H44, H128 and E266 may directly coordinate Zn or, alternatively, help in shaping the 3D structure of the Zn binding site by holding coordinating groups in correct position. The second interpretation is the most intuitive explanation for the large effect of a positively charged amino acid like K233. However, participation of lysine as a direct coordinating group has been demonstrated in the binuclear metal centers of several Zn- or Ni-containing enzymes. Two mechanisms have been advanced as explanations of this counter-intuitive phenomenon. In the first one, the ε amine of the lysine is carbamylated, i.e. the positively charged amine group is modified to a negatively charged carbamate group upon reaction with carbon dioxide (Volbeda et al., 1996). In some cases this reaction requires the presence of

chaperone proteins (Park and Hausinger, 1995) and the unstable carbamate group is stabilized by the constitutively bound Zn or Ni cation. Such a mechanism appears inappropriate for a modulatory Zn binding site where occupancy by the metal cation must be transient. In the second mechanism, the unprotonated form of the ε amine coordinates the divalent ion (Burley et al., 1992; Buy et al., 1996). To achieve deprotonation of the lysine lateral chain (usual pKa around 10), a two step binding process may occur in which the divalent metal binds first to other "classical" determinants of the binding site (like histidines) bringing the divalent cation close to the ε amine deprotonating it. The deprotonated amine would then bind to the metal ion. This mechanism seems more appropriate to account for the reversible Zn binding on modulatory sites. In the NR2A LIVBP-like domain, H44 and H128 (and possibly E266) may be the determinants involved in the first step allowing approach of K233 by the partly coordinated Zn ion.

In contrast with Choi and Lipton (1999), our data suggest a modest role for NR2A-H42 at the high-affinity Zn binding site. The mutant H42A produces a moderate shift in Zn IC_{50} (11 fold). Choi and Lipton (1999) observed a much larger shift (211 fold) with the mutation NR2A-H42G. Participation of both H42 and H44 seems appealing given the frequency of shortly spaced histidines known to occur in Zn binding sites. However, if H42 were participating in Zn coordination, substitution of the histidine by alanine should result in a Zn binding perturbation as large as that due to substitution by glycine. We therefore propose that H42 does not directly coordinate the Zn ion. Due to its very close proximity with H44, it may be involved in the correct positioning of H44 with regards to H128. Indeed a short spaced histidine residue in the Zn center of alkaline phosphatase serves just such a function by forming a hydrogen bond that helps to correctly position a Zn coordinating residue (Kim and Wyckoff, 1991). H42G most likely introduces a much larger steric change than H42A and thus possibly a larger displacement of H44.

Whatever the actual role of the four potential determinants of the Zn binding site (coordination or local structure), they must be located close to each other in the 3D structure of the LIVBP-like domain. There is no available structural data for the LIVBP-like domain of ionotropic glutamate receptors unlike the ligand binding domain which has been purified and crystallized in the case of GluR2 (Armstrong et al., 1998), an AMPA glutamate receptor. However, the 3D structures of different members of the bacterial LIVBP family have been solved. LIVBP consists of two lobes connected via a hinge to form a gorge containing the amino acid binding site. The amino acid binds

to residues contributed by each of the two lobes promoting closure of the gorge. Given their scattered localization along the LIVBP-like domain sequence, a tempting hypothesis is that all four residues, H44, H128, K233 and E266 belong to loops (separating secondary structure elements) that flank the gorge from both lobes (lobe 1 for H44 and H128 and lobe 2 for K233 and E266 for example). Such a localization would allow an appealing mechanism for Zn inhibition in which Zn, by binding to determinants on both lobes, might promote the closure of the gorge. If such an hypothesis were experimentally verified, a further step in understanding the Zn inhibition mechanism could be to identify the interaction domains that signal to the rest of the protein the change of conformation associated with the closure of the gorge .

EXPERIMENTAL PROCEDURES

NMDA receptor subunit constructs and heterologous expression

Wild type and mutant constructs: The pcDNA3 expression plasmids for Rat NR1a (hereon simply referred to as NR1), NR2A and NR2C subunits have been described in Paoletti et al. (1997). Point mutations were produced according to the method of Kunkel (1985). For each mutation, at least two independent clones were isolated, in which the presence of the mutation was verified by sequencing across the mutated region (~50 bp on either side of the mutation). For those mutations resulting in a phenotype that differed from wild type (according to our Zn inhibition screening procedure, see results), the two independent clones were functionally characterized to confirm that the modified phenotype resulted from the planned mutation rather than from a stray mutation produced during the mutagenesis process.

Chimeric constructs: most of the NR2A/NR2C chimeras used in this study have already been described in Villarroel et al., (1998). They were obtained by swapping homologous domains from one subunit into the other after introducing convenient restriction sites by PCR. NR2A/C(553), NR2C/A(564) and NR2C(AN1-4) contain only wild type amino acid sequences. In NR2A/C(553), the N-terminal region of NR2A up to P552 is followed by the NR2C sequence starting at Y564 (switch at position 553). In NR2C/A(564), the switch is between NR2C-P563 and NR2A-F553 (564th position). In NR2C(AN1-4) the switch is between NR2A-E413 and NR2C-R424. The other chimeras used in this study have been generated using NR2A' as the receiving subunit. NR2A' differs from wild type NR2A in two respects: first, the four residues just preceeding TM1 (F553 to S556 in NR2A) have been replaced by their NR2C homologues (Y564 to A567); second, two non-silent restriction sites have been introduced leading to the mutations K221Q, I222V, S384Y and L385M. Borders of the different N1a to N6 N-terminal regions are as follows (given in NR2A/NR2C amino acid position): K138/K146 end of N1a; L219/L229 end of N1b (and N1); T342/T352 end of N2; L383/L393 end of N3; E413/E423 end of N4; K465/K476 end of N5 and P552/P563 end of N6. In all deletion constructs, the NR2A N-terminal signal sequence was conserved. In addition to the N-terminal deletion of the N1-N3 segments, the deletion construct NR2A'(ΔN1-3)tr, has a deletion of part of the C-terminal introduced by insertion of a stop codon at position NR2A'-K1116.

Heterologous expression of NMDA receptors in Xenopus oocytes: 20 nl of a mixture of NR1 and NR2 plasmids (ratio 1/2) at a final concentration of 10 ng/µl were injected into the oocyte nuclei. Oocytes were prepared and kept as described in Paoletti et al. (1995) and recorded 1 to 5 days following DNA injection. Most of this work consisted in functional characterization of chimeric or mutant NR2 subunits. In the *Xenopus* oocyte, heterologous expression of the recombinant NR1 subunit only has been shown to result in measurable glutamate responses ("homomeric" NR1 responses). due to activation of receptors made from heterologous NR1 subunits associated with endogenous *Xenopus* NR subunits (see Soloviev et al., 1996). All our NR2 constructs were tested by coexpression with wild type NR1 subunits. We were therefore concerned by the possibility that some of our chimeric or mutant NR2 constructs might not be functional and display an "homomeric" NR1 phenotype. However, under our experimental conditions (0.3 mM Ba^{2+} as the sole external divalent), the amplitude of "homomeric" NR1 responses never exceeds 50 nA at -60 mV, even 5 days after cDNA injection. All the NR2 constructs tested in this study, except NR2A'(CN1) (see Results) induced responses that were at least 5 fold larger than the largest "homomeric" NR1 response. We thus conclude that all these constructs participated in the formation of functional NR1/NR2 receptors.

Buffering solutions for Zn^{2+}, Ni^{2+} and H^{+}

Zn buffered solutions: NMDA receptors containing NR2Awt have such a high affinity for Zn that they are tonically inhibited by trace concentrations of contaminating Zn in standard solutions (Paoletti et al., 1997). In order to make Zn inhibition dose-response curves in the submicromolar range, the Zn concentration must be buffered using chelators of moderate affinity. Tricine (N-tris[Hydroxymethyl]methylglycine) with constants $K_1 = 10^{-5}$ M for the equilibrium M + L <=> ML, and $K_2 = 10^{-3}$ M for the equilibrium ML + L <=> ML_2 (Vieles et al., 1972; see also Paoletti et al., 1997) was added at 10 mM to buffer Zn in the range 1 nM - 1 µM. ADA (N-[2-acetamido]iminodiacetic acid) with $K_1 = 10^{-7.3}$ M and $K_2 = 10^{-2.2}$ M (Martell and Smith, 1989) was added at 1 mM to buffer Zn in the 0.05 -100 nM range. Geochem, a multi-purpose chemical speciation program (Parker et al., 1995) was used to establish the relation between the concentrations of free and total Zn contained in the buffered solutions ($[Zn]_f$ and $[Zn]_t$,

respectively). Equilibria taken into account were the ones between chelators and Zn, the ones between chelators and protons and the ones between Zn^{2+} and OH^- (equilibria between Zn and either glutamate or glycine, both present at 100 µM, were neglected). At pH 7.3 and with 10 mM tricine, calculations show that there is a linear relation $[Zn]_f = [Zn]_t/200$ for $[Zn]_f < 1$ µM. A linear relation, $[Zn]_f = [Zn]_t/17000$, was also found at pH 7.3 with 1 mM ADA for $[Zn]_f < 3$ nM; for larger $[Zn]_f$ (10, 30 and 100 nM), calculated $[Zn]_t$ were 150, 350 and 640 µM respectively. For all Zn inhibition dose-response curves, a Zn-free reference solution was made by adding 10 µM DTPA (diethylenetriamine-pentaacetic acid, a strong Zn chelator, $K_D = 10^{-15.6}$ M) to the zero-added Zn buffered solution.

Ni buffered solutions: Ni inhibition in NR2A-containing receptors requires submillimolar Ni concentrations. With such high Ni concentrations, complexes between Ni and glutamate or glycine must be taken into consideration. Using Geochem (with $K_1 = 10^{-5.6}$ M and $K_2 = 10^{-4.2}$ M for glutamate; $K_1 = 10^{-5.75}$ M and $K_2 = 10^{-4.85}$ M for glycine), we calculated total concentrations of Ni, glutamate and glycine that were appropriate to obtain a constant 100 µM concentration for free glutamate and glycine, and three different concentrations of free Ni, 10 µM, 100 µM and 1 mM. For the three cases, the calculated concentrations were (in µM): 101, 110 and 190 for glutamate; 102, 122 and 310 for glycine; 13, 130 and 1300 for Ni. For each tested concentration of Ni, a control solution without agonist was obtained by simply adding Ni at the final desired concentration to our normal control solution.

pH buffered solutions: in the proton inhibition experiments, 5 mM MES (2[N-Morpholino]ethanesulfonic acid, $pK_a = 6.1$), 5 mM HEPES (N-[2-Hydroxyethyl]piperazine-N'-[2-ethane-sulfonic acid, $pK_a = 7.5$) and 10 mM tricine ($pK_a = 8.2$) were present in the bath solutions to allow pH buffering on a wide range (5.8 to 8.3). pH was adjusted with NaOH. 10 µM DTPA was added to all solutions used in proton inhibition experiments in order to achieve Zn-free conditions. Agonists were used at saturating 100 µM concentrations.

All chemicals except $NiCl_2$ were purchased from Sigma (Saint Quentin Fallavier, France). Zn and Ni were added as chloride salts ($ZnCl_2$, ACS reagent quality; $NiCl_2$, Puratonic quality, purchased from Alfa Aesar, Karlsruhe, Germany) by dilution from 1M stock solutions prepared in 0.1M HCl.

Recording and data analysis

Recording conditions: two-electrode voltage-clamp and superfusion system have already been described previously (Paoletti et al., 1997). Bath solutions always contained (in mM): 100 NaCl, 2.8 KCl, 5 HEPES and 0.3 $BaCl_2$, pH adjusted to 7.3 with NaOH (except in proton inhibition experiments). The low Ba concentration was chosen as a compromise between the necessity of having divalents in the recording solutions to reduce endogenous currents through cationic channels activated in divalent free solution and the minimisation of chloride currents through endogenous Ca-activated channels (see Weber, 1999).

Currents activated by application of the agonists (glutamate and glycine both applied at a saturating dose of 100 μM) were recorded either at a steady state voltage of -60 mV, or during 4 s -100/+50 mV voltage ramps (in this latter case, both capacitive and leakage currents were recorded before each application of agonist and subtracted from the traces recorded in the presence of the agonists). A voltage-ramp protocol is required to separate Zn voltage-independent inhibition and Zn voltage-dependent block when Zn concentrations exceed 3 μM (see Paoletti et al., 1997). The same voltage-ramp protocol was used to study the inhibition by Ni, which, like Zn, also induces a voltage-dependent block in NMDA receptors (Paoletti and Neyton, in preparation).

Spontaneous run-down of the responses to agonist was often a problem in the long experiments required to establish dose-response curves. To circumvent this difficulty, each response under test conditions was generally bracketed by two responses under reference conditions (Zn-free solution for Zn inhibition curves, no-added Ni for Ni inhibition curves and pH 8.3 for proton inhibition curves, respectively). The relative current under a particular test condition was calculated as the ratio between the current measured in the test condition and the mean of the reference currents recorded just before and after the test current.

Data analysis: full dose-response curves were obtained in a minimum of three different oocytes for each studied construct. Experimental points of dose-response curves shown in figures 1, 4 and 5 correspond to the means of the relative currents. Error bars represent standard deviations. Lines correspond to the best fit performed with the Sigmaplot fitting procedure using the following equations:

$$f(x) = 1 - a / [1 + (IC_{50} / x)^n] \qquad [1]$$

for Zn and Ni inhibitions (x is the Zn or Ni concentration, a is the maximal inhibition and n is the Hill coefficient);

$$f(x) = 1 / [1 + (10^{pH - pHI50})^n] \quad [2]$$

for proton inhibition;

$$f(x) = 1 / [1 + (EC_{50} / x)^n] \quad [3]$$

for glutamate and glycine activation curves [f(x) is the relative current normalized to the maximum current recorded at saturating 100 μM concentrations of both agonists; x is the concentration of the tested agonist, the other one being present at 100 μM; n is the Hill coefficient]. In fitting the glycine activation curves, errors potentially introduced by contaminating glycine (Johnson and Ascher, 1987) were eliminated by restricting the fit to experimental points obtained with at least 300 nM glycine. In Table II, inhibition curves for each individual oocyte was fitted and the value given for IC_{50}, maximal inhibition and Hill coefficient are means ± SD calculated from parameter values of the individual fits. Table III was constructed in the same way.

ACKNOWLEDGEMENTS

This work was supported by grants from the EEC (BMH4 CT97 2374) and from DGICYT (PM96-0008 to J.L.). A.F. was funded by a Chateaubriand fellowship from the French Government and by the Fondation pour la Recherche Médicale. We thank Pierre Paoletti and Philippe Ascher for helpful discussions along the project and for their comments on the manuscript.

REFERENCES

Armstrong, N., Sun, Y., Chen, G. Q., and Gouaux, E. (1998). Structure of a glutamate-receptor ligand-binding core in complex with kainate. Nature *395*, 913-917.

Burley, S. K., David, P. R., Sweet, R. M., Taylor, A., and Lipscomb, W. N. (1992). Structure determination and refinement of bovine lens leucine aminopeptidase and its complex with bestatin. J. Mol. Biol. *224*, 113-140.

Buy, C., Girault, G., and Zimmermann, J. L. (1996). Metal binding sites of H(+)-ATPase from chloroplast and Bacillus PS3 studied by EPR and pulsed EPR spectroscopy of bound manganese(II). Biochemistry *35*, 9880-9891.

Chen, N., Moshaver, A., and Raymond, L. A. (1997). Differential sensitivity of recombinant N-methyl-D-aspartate receptor subtypes to zinc inhibition. Mol. Pharmacol. *51*, 1015-1023.

Choi, Y.-P., and Lipton, S. A. (1999). Identification and mechanism of action of two histidine residues underlying high-affinity Zn^{2+} inhibition of the NMDA receptor. Neuron *23*, 171-180.

Christianson, D. W. (1991). Structural biology of zinc. Adv. Protein Chem. *42*, 281-355.

Christine, C. W., and Choi, D. W. (1990). Effect of zinc on NMDA receptor-mediated channel currents in cortical neurons. J. Neurosci. *10*, 108-116.

Colquhoun, D. (1998). Binding, gating, affinity and efficacy: the interpretation of structure-activity relationships for agonists and of the effects of mutating receptors. Br. J. Pharmacol. *125*, 924-947.

Dingledine, R., Borges, K., Bowie, D., and Traynelis, S. (1999). The glutamate receptor ion channels. Pharmacol. Rev. *51*, 7-61.

Glusker, J. P. (1991). Structural aspects of metal liganding to functional groups in proteins. Adv. Protein Chem. *42*, 1-76.

Harvey, R. J., Thomas, P., James, C. H., Wilderspin, W., and Smart, T. G. (1999). Idendtification of an inhibitory Zn^{2+} binding site on the human glycine receptor $\alpha 1$ subunit. J. Physiol. *520*, 53-64.

Horenstein, J., and Akabas, M. H. (1998). Location of a high affinity Zn^{2+} binding site in the channel of $\alpha_1 ß_1$ γ-aminobutyric $acid_A$ receptors. Mol. Pharmacol. *53*, 870-877.

Ishii, T., Moriyoshi, K., Sugihara, H., Sakurada, K., Kadotani, H., Yokoi, M., Akazawa, C., Shigemoto, R., Mizuno, N., Masu, M., and Nakanishi, S. (1993). Molecular characterization of the family of the N-methyl-D-aspartate receptor subunits. J. Biol. Chem. *268*, 2836-2843.

Johnson, J. W., and Ascher, P. (1987). Glycine potentiates the NMDA response in cultured mouse brain neurons. Nature *325*, 529-531.

Karlin, S., and Zhu, Z. Y. (1997). Classification of mononuclear zinc metal sites in protein structures. Proc. Natl. Acad. Sci. USA *94*, 14231-14236.

Kashiwagi, K., Fukuchi, J., Chao, J., Igarashi, K., and Williams, K. (1996). An aspartate residue in the extracellular loop of the N-methyl-D-aspartate receptor controls sensitivity to spermine and protons. Mol. Pharmacol. *49*, 1131-1141.

Kashiwagi, K., Pahk, A. J., Masuko, T., Igarashi, K., and Williams, K. (1997). Block and modulation of N-methyl-D-aspartate receptors by polyamines and protons: role of amino acid residues in the transmembrane and pore-forming regions of NR1 and NR2 subunits. Mol. Pharmacol. *52*, 701-713.

Kim, E. E., and Wyckoff, H. W. (1991). Reaction mechanism of alkaline phosphatase based on crystal structures. Two-metal catalysis. J. Mol. Biol. *218*, 449-464.

Köhr, G., Eckhardt, S., Lüddens, H., Monyer, H., and Seeburg, P. H. (1994). NMDA receptor channels: subunit-specific potentiation by reducing agents. Neuron *12*, 1031-1040.

Krupp, J. J., Vissel, B., Heinemann, S. F., and Westbrook, G. L. (1998). N-terminal domains in the NR2 subunit control desensitization of NMDA receptors. Neuron *20*, 317-327.

Kuner, T., Wollmuth, L. P., Karlin, A., Seeburg, P. H., and Sakmann, B. (1996). Structure of the NMDA receptor channel M2 segment inferred from the accessibility of substituted cysteines. Neuron *17*, 343-352.

Kunkel, T. A. (1985). Rapid and efficient site-specific mutagenesis without phenotypic selection. Proc. Natl. Acad. Sci. U.S.A. *82*, 488-492.

Laube, B., Kuhse, J., Rundström, N., Kirsch, J., Schmieden, V., and Betz, H. (1995). Modulation by zinc of native rat and recombinant human inhibitory glycine receptors. J. Physiol. *483*, 613-619.

Legendre, P., and Westbrook, G. L. (1990). The inhibition of single N-methyl-D-aspartate-activated channels by zinc ions on cultured rat neurones. J. Physiol. *429*, 429-449.

Li, C., Peoples, R. W., and Weight, F. F. (1997). Inhibition of ATP-activated current by zinc in dorsal root ganglion neurones of bullfrog. J. Physiol. *505*, 641-653.

Lippard, S. J., and Berg, J. M. (1997). Principes de biochimie minérale (Paris and Brussels: DeBoeck et Larcier).

Martell, A. E., and Smith, R. M. (1989). Critical Stability Constants, Volume 1-6 (New York: Plenum).

Masuko, T., Kashiwagi, K., Kuno, T., Nguyen, N. D., Pahk, A. J., Fukuchi, J., Igarashi, K., and Williams, K. (1999). A regulatory domain (R1-R2) in the amino terminus of the N-methyl-D-aspartate receptor: effects of spermine, protons, and ifenprodil, and structural similarity to bacterial leucine/isoleucine/valine binding protein. Mol. Pharmacol. *55*, 957-969.

McBain, C., and Mayer, M. (1994). N-methyl-D-aspartic acid receptor structure and function. Physiol. Rev. *74*, 723-760.

Nakanishi, N., Shneider, N. A., and Axel, R. (1990). A family of glutamate receptor genes: evidence for the formation of hetero-multimeric receptors with distinct channel properties. Neuron *5*, 569-581.

O'Hara, P. J., Sheppard, P. O., Thogersen, H., Venezia, D., Haldeman, B. A., McGrane, V., Houamed, K. M., Thomsen, C., Gilbert, T. L., and Mulvihill, E. R. (1993). The ligand-binding domain in metabotropic glutamate receptors is related to bacterial periplasmic binding proteins. Neuron *11*, 41-52.

Paoletti, P., Ascher, P., and Neyton, J. (1997). High-affinity zinc inhibition of NMDA NR1-NR2A receptors. J. Neurosci. *17*, 5711-5725.

Paoletti, P., Neyton, J., and Ascher, P. (1995). Glycine-independent and subunit-specific potentiation of NMDA responses by extracellular Mg2+. Neuron *15*, 1109-1120.

Park, I. S., and Hausinger, R. P. (1995). Requirement of carbon dioxide for in vitro assembly of the urease nickel metallocenter. Science *267*, 1156-1158.

Parker, D. R., Norvell, W. A., and Chaney, R. L. (1995). GEOCHEM-PC: A chemical speciation program for IBM and compatible personal computers. In Chemical equilibrium and reaction models., R. H. Loeppert and e. al., eds. (Madison, WI: ASA and SSSA).

Schneggenburger, R., and Ascher, P. (1997). Coupling of permeation and gating in an NMDA-channel pore mutant. Neuron *18*, 167-177.

Soloviev, M. M., Brierley, M. J., Shao, Z. Y., Mellor, I. R., Volkova, T.M., Kamboj, R., Ishimaru, H., Sudan, H., Harris, J., Foldes, R. L., Grishin, E.V., Usherwood, P. N. R., and Barnard, E. A. (1996). Functional expression of a recombinant unitary glutamate receptor from *Xenopus*, which contains N-methyl-D-aspartate (NMDA) and non-NMDA receptor subunits. J. Biol. Chem. *271*, 32572-32579.

Stern-Bach, Y., Bettler, B., Hartley, M., Sheppard, P. O., O'Hara, P. J., and Heinemann, S. F. (1994). Agonist selectivity of glutamate receptors is specified by two domains structurally related to bacterial amino-acid proteins. Neuron *13*, 1345-1357.

Sullivan, J., Traynelis, S., Chen, H., Escobar, W., Heinemann, S., and Lipton, S. (1994). Identification of two cysteine residues that are required for redox modulation of the NMDA subtype of glutamate receptor. Neuron *13*, 929-936.

Traynelis, S. F., Burgess, M. F., Zheng, F., Lyuboslavsky, P., and Powers, J. L. (1998). Control of voltage-independent zinc inhibition of NMDA receptors by the NR1 subunit. J. Neurosci *18*, 6163-6175.

Traynelis, S. F., and Cull-Candy, S. G. (1990). Proton inhibition of N-methyl D-aspartate receptors in cerebellar neurons. Nature *345*, 347-350.

Vallee, B.L., and Auld, D.S. (1993) Cocatalytic zinc motifs in enzyme catalysis. Proc. Natl. Acad. Sci. USA *90*, 2715-2718.

Vieles, P., Frezou, C., Galsomias, J., and Bonniol, A. (1972). Etude physicochimique de la tricine et de ses complexes avec les ions de transition Co II, Ni II, Cu II, Zn II. J. Chim. Phys., Physiochim. Biol. *69*, 869-874.

Villarroel, A., Regalado, M. P., and Lerma, J. (1998). Glycine-independent NMDA rReceptor desensitization: localization of structural determinants. Neuron *20*, 329-339.

Volbeda, A., Fontecilla-Camps, J. C., and Frey, M. (1996). Novel metal sites in protein structures. Curr. Opin. Struct. Biol. *6*, 804-812.

Weber, W. M. (1999). Endogenous ion channels in oocytes of *Xenopus laevis*: recent developments. J. Membr. Biol. *170*, 1-12.

Williams, K. (1996). Separating dual effects of zinc at recombinant N-methyl D-aspartate receptors. Neurosci. Lett. *215*, 9-12.

Williams, K., Kashiwagi, K., Fukuchi, J., and Igarashi, K. (1995). An acidic amino acid in the N-methyl-D-aspartate receptor that is important for spermine stimulation. Mol. Pharmacol. *48*, 1087-1098.

Wooltorton, J. R. A., McDonald, B. J., Moss, S. J., and Smart, T. G. (1997). Identification of a Zn^{2+} binding site on the murine $GABA_A$ receptor complex: dependence on the second transmembrane domain of ß subunits. J. Physiol. *505*, 633-640.

Zheng, X., Zheng, L., Wang, A. P., Araneda, R. C., Lin, Y., Zukin, R. S., and Bennett, M. V. (1999). Mutation of structural determinants lining the N-methyl-D-aspartate receptor channel differentially affects phencyclidine block and spermine potentiation and block. Neuroscience *93*, 125-134.

FIGURE LEGENDS

FIGURE 1. The N-terminal region preceding the TM1 segment of the NR2A subunit confers high-affinity Zn inhibition to NMDA receptors.

A: current responses induced by applications of 100 μM of glutamate and glycine in oocytes expressing NMDA receptors containing wild type NR2A (A1), wild type NR2C (A2), or chimeric NR2A/NR2C subunits (A3 and A4). The recordings were made at -60 mV either in the presence of 50 nM buffered Zn (*) or in the absence of Zn (10 μM DTPA in the bath). The bar above the current traces indicates agonist application. A schematic diagrams of the NR2 construct is shown in each panel using white and black boxes for NR2A and NR2C regions, respectively.

B: Zn dose-response curves of the constructs shown in A. To avoid contamination of the Zn voltage-independent inhibition by Zn voltage-dependent block all current measurements were made at the end of a 4 s voltage ramp from -100 mV to +50 mV. The relative current is the ratio between leak-subtracted currents recorded in the presence and absence of Zn, respectively. Zn was buffered using 10 mM tricine for [Zn] ≤ 1 μM (see Experimental Procedures). Experimental points were fitted using equation 1 (solid lines). Parameters of the fits are given in the text.

FIGURE 2. The high affinity Zn binding site can be localized to the LIVBP-like domain of the N-terminal of NR2A receptors.

The left hand side of the figure shows schematic diagrams of different chimeric and deletion constructs of the NR2 subunit. The precise location of the fragments borders is given in the Experimental Procedures section. Apparent Zn affinities (IC_{50}s) measured with receptors containing each of the constructs (mean of at least three independent determinations) is shown on the right. The region within ± 5-fold of the mean apparent affinity of wild type NR1-NR2A receptors is indicated by the hashed box.

FIGURE 3. Mutagenesis scans to identify residues important for Zn binding.

Alignment of NR2A, NR2B, NR2C and NR2D sequences has been taken from Ishii et al. (1993). The N-terminal signal sequences are omitted. Putative Zn ligands of the high affinity Zn binding site (H, C, D or E residues that were present in NR2A but not conserved at homologous positions in

NR2C) were mutated in the first mutagenesis series (triangles). A second mutagenesis scan was performed through the NR2A LIVBP-like domain to target putative Zn coordinating residues that were conserved between NR2A and NR2C subunits (diamonds). Some NR2A positively charged residues have also been mutated in that series. Bold residues indicate positions where mutations "moderately" affected Zn inhibition (see text). Boxed residues indicate positions where mutations resulted in a "strong" effect on the apparent Zn affinity.

FIGURE 4. "Strong" mutations cause large shifts in Zn affinity.

Zn dose-response curves obtained in oocytes expressing NMDA receptors containing NR2A "strong" mutants. Relative currents were measured at +50 mV as indicated in Fig.1B. The values for the IC50, maximal inhibition and Hill coefficient obtained from the fits for each of the mutants are given in table II.

FIGURE 5. Voltage-independent inhibition due to either H^+ or Ni^{2+} ions is not affected by mutations at NR2AH44, NR2AH128, NR2AK233 and NR2AE266.

A: The responses of oocytes expressing each of the "strong" NR2A mutants as well as wild type, two NR1 pore mutants and one "moderate" NR2A mutant receptors were recorded at different pH values and at -60 mV in the absence of Zn (10 mM tricine and 10 μM DTPA were present in all solutions). The experimental points were fitted with equation 2 (see Experimental Procedures) giving the following values for the fitting parameters (pHI_{50} and n_H respectively): 6.8 and 1.6 for NR1wt/NR2Awt (•); 6.8 and 1.6 for NR1wt/NR2A-H44A (□); 6.7 and 1.5 for NR1wt/NR2A-H128S (♦); 6.7 and 1.4 for NR1wt/NR2A-K233R (o); 6.7 and 1.4 for NR1wt/NR2A-E266S (▼). The curves for the "strong" mutants were not very different from that obtained with wild-type receptors. In contrast the pH-response curves for the pore mutants NR1-W590C/NR2Awt (▽) and NR1-N598C/NR2Awt (■) showed markedly less sensitivity to protons (pHI_{50} and n_H were 6.0 and 2.0, 6.2 and 1.9 respectively), whereas the pH curve of the "moderate" mutant NR1wt/NR2A-R244G (◊) showed a clear increase in proton sensitivity (pHI_{50} = 7.1 and n_H = 1.7).

B: The Ni sensitivity of a similar series of NMDA receptors was measured with Ni buffered solutions (see Experimental Procedures). Current measurements were made at the end of a 4 s voltage ramp from -100mV to +50 mV to avoid contamination of the Ni voltage-independent inhibition by Ni

voltage-dependent block. Experimental points were fitted by equation 1 imposing $n_H = 1$. Symbols as in A except for (▼) which corresponds to NR1wt/NR2A-E266A receptors. Dose-response curves for NR1wt/NR2Awt and two of the "strong" mutant receptors NR1wt/NR2A-K233R and NR1wt/NR2A-E266A are very similar (IC_{50} and maximal inhibition being respectively 99 μM and 0.92 for NR2Awt; 97 μM and 0.85 for NR2A-K233R; 82 μM and 0.89 for NR2A-E266A). For NR1wt/NR2A-H44A and NR1wt/NR2A-H128S receptors, only one Ni concentration was tested (see text). The Ni dose-response curves for NR1-W590C/NR2Awt and NR1-N598C/NR2Awt receptors showed a decreased apparent affinity (550 μM and 500 μM respectively) and a lower maximal inhibition (0.70 and 0.60 respectively).

NR2A construct	relative current 50 nM Zn (%)	relative current 500 nM Zn (%)	n
wt	43 ± 6	30 ± 5	31
H42A	**79 ± 2**	**41 ± 3**	3
H44A	**99 ± 1**	**78 ± 3**	3
D45N	45 ± 5	32 ± 5	3
E48A-R49A-E50Q	43 ± 2	29 ± 3	3
D78A	**80 ± 3**	**52 ± 6**	3
H85S	34 ± 5	26 ± 5	3
C87A	51 ± 7	38 ± 7	2
D88S	39 ± 6	26 ± 6	3
H96A	42 ± 3	27 ± 3	5
H128S	**99 ± 1**	**92 ± 2**	3
Q163E-D164E	46 ± 5	31 ± 4	3
H168A	38 ± 4	25 ± 3	6
D182S	37 ± 1	28 ± 2	3
D192N	42 ± 6	34 ± 7	3
D207A	**77 ± 1**	**52 ± 1**	3
E211Q	**64 ± 2**	**44 ± 3**	5
D212N	39 ± 2	32 ± 1	3
K214A	35 ± 7	31 ± 6	3
H223G	40 ± 7	27 ± 4	6
C231A	45 ± 3	30 ± 3	3
K233R	**100 ± 1**	**90 ± 5**	3
K233S	**93 ± 3**	**81 ± 3**	3
D234A	36 ± 2	26 ± 2	4
E235Q	46 ± 7	35 ± 7	3
E242Q	45± 5	34 ± 5	3
R244G	**23 ± 1**	**23 ± 1**	3
D252N	46 ± 5	nd	4
E266A	**98 ± 2**	**85 ± 4**	3
E266S	**98 ± 2**	**90 ± 4**	3
K270A	40 ± 1	nd	3
E271S	45 ± 7	33 ± 5	3
D285S	44 ± 5	31 ± 4	3
E289Q	41 ± 12	nd	7
E308Q	41 ± 11	nd	8
C320A	49 ± 6	32 ± 4	3
E328Q	40 ± 12	nd	6
H332S-H335S	43 ± 14	nd	6
E352P-E353G	49 ± 2	31 ± 5	3
H358A	**56 ± 6**	**38 ± 5**	5
E371Q	38 ± 11	nd	6
E373A	34 ± 3	23 ± 2	2
K374S	**85 ± 6**	**63 ± 10**	6
H387S	38 ± 9	29 ± 3	6
C399A	41 ± 5	nd	3

Table I : screening for effects on the high affinity Zn inhibition due to substitution of H, C, D or E residues and positively charged K or R residues within the NR2A LIVBP-like domain. Constructs and figures that differ from NR2Awt by more than 1.25-fold are in bold; those that differ by more than 2-fold are underlined.

	NR2 construct	IC_{50}, nM	I_{max}	n_{Hill}	n
a	NR2Awt	16 ± 6	0.77 ± 0.02	0.87 ± 0.17	11
b	NR2Cwt	25000 ± 5000	0.97 ± 0.03	0.73 ± 0.05	9
c	NR2A-H44A	1100 ± 100	0.78 ± 0.03	1.64 ± 0.36	7
d	NR2A-H128S	8300 ± 600	0.96 ± 0.03	1.13 ± 0.07	4
e	NR2A-K233R	3100 ± 300	0.82 ± 0.04	0.90 ± 0.12	3
f	NR2A-E266S	6800 ± 600	0.99 ± 0.01	1.07 ± 0.15	3
g	NR2A-E266A	1400 ± 500	0.80 ± 0.05	0.84 ± 0.13	3
h	NR2A-H42A	180 ± 30	0.85 ± 0.03	1.00 ± 0.05	4
i	NR2A-D78A	210 ± 40	0.81 ± 0.03	0.79 ± 0.12	5
j	NR2A-D207A	170 ± 80	0.84 ± 0.10	0.65 ± 0.08	10
k	NR2A-E211Q	80 ± 50	0.79 ± 0.02	0.70 ± 0.05	6
l	NR2A-H358A	32 ± 3	0.81 ± 0.01	0.82 ± 0.08	3
m	NR2A-K374S	400 ± 90	0.82 ± 0.05	0.72 ± 0.06	4
n	NR2A-R244G	0.46 ± 0.10	0.80 ± 0.01	1.15 ± 0.16	3
o	NR2A-H42A-H44A	2600 ± 400	0.88 ± 0.06	2.03 ± 0.49	3
p	NR2A-H42A-H44A-E266A	4000 ± 300	0.92 ± 0.04	1.39 ± 0.03	2

Table II : parameters of voltage-independent Zn inhibition curves obtained in oocytes expressing either wild type NR2 constructs (rows a and b), or NR2A mutants showing a large decrease (rows c to g), a moderate decrease (rows h to m) or an increase (row n) in their apparent affinity for Zn. Rows o and p correspond to multiple mutations.

construct	Glutamate		Glycine	
	EC_{50}, µM	n_{Hill}	EC_{50}, µM	n_{Hill}
NR1wt/2Awt	5.9 ± 0.5	1.4 ± 0.1	1.4 ± 0.4	1.5 ± 0.1
NR1wt/NR2A-H44A	4.4 ± 1.0	1.3 ± 0.1	1.3 ± 0.1	1.5 ± 0.1
NR1wt/NR2A-H128S	3.8 ± 0.9	1.3 ± 0.1	1.3 ± 0.1	1.5 ± 0.1
NR1wt/NR2A-K233R	6.0 ± 0.4	1.4 ± 0.1	1.5 ± 0.3	1.7 ± 0.3
NR1wt/NR2A-E266A	5.9 ± 0.5	1.4 ± 0.1	1.5 ± 0.3	1.9 ± 0.3
NR1wt/NR2A-R244G	3.7 ± 0.3	1.3 ± 0.1	1.9 ± 0.1	1.5 ± 0.1
NR1-W590C/NR2Awt	0.54 ± 0.06	1.5 ± 0.3	0.17 ± 0.02	1.8 ± 0.3
NR1-N598C/NR2Awt	0.47 ± 0.08	1.5 ± 0.2	0.29 ± 0.02	2.6 ± 0.4

Table III : parameters of glutamate and glycine activation curves of wild type and mutant receptors. Responses were recorded at a steady negative voltage (-30 mV or -60 mV) with solutions containing 10 mM tricine, 10 µM DTPA and no added Zn (Zn-free conditions) in three different oocytes for each construct except for glycine activation curve of NR1wt/NR2A-E266A which was obtained in two cells only.

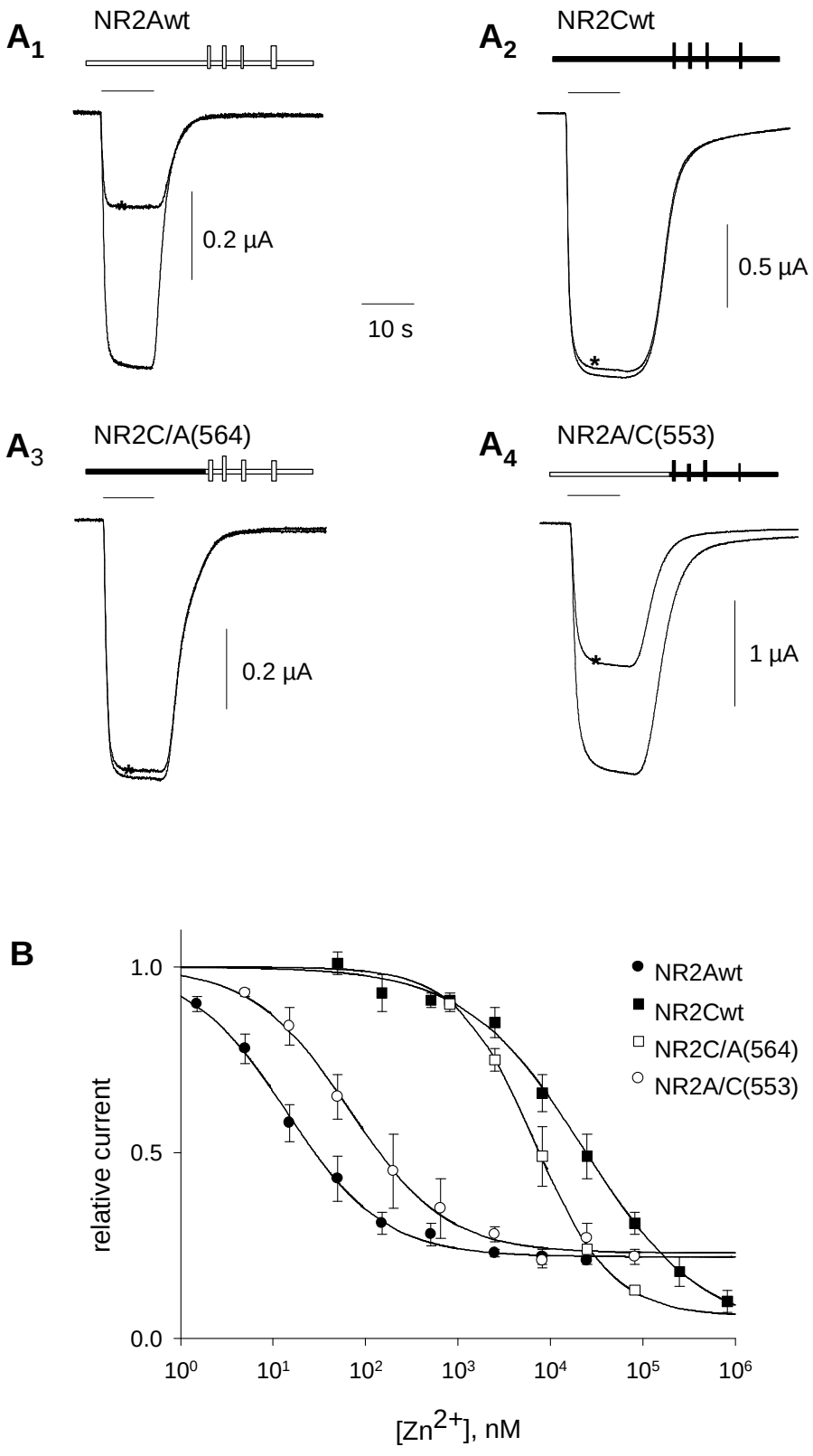
A1
NR2Awt
0.2 µA
10 s
A2
NR2Cwt
0.5 µA
A3
NR2C/A(564)
0.2 µA
A4
NR2A/C(553)
1 µA
B
relative current
1.0
0.5
0.0
NR2Awt
NR2Cwt
NR2C/A(564)
NR2A/C(553)
10^0
10^1
10^2
10^3
10^4
10^5
10^6
[Zn2+], nM

Figure 1

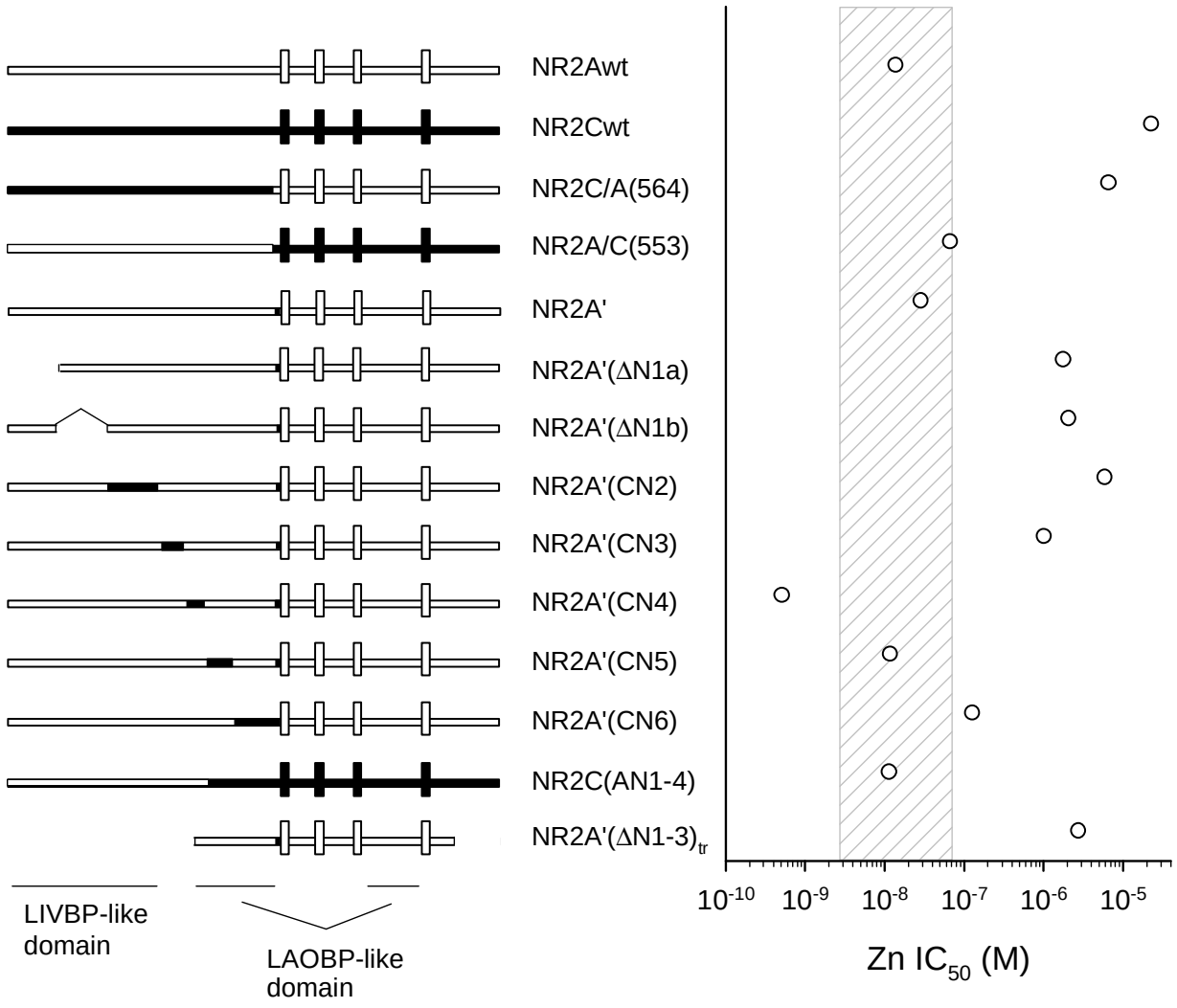
NR2Awt
NR2Cwt
NR2C/A(564)
NR2A/C(553)
NR2A'
NR2A'(ΔN1a)
NR2A'(ΔN1b)
NR2A'(CN2)
NR2A'(CN3)
NR2A'(CN4)
NR2A'(CN5)
NR2A'(CN6)
NR2C(AN1-4)
NR2A'(ΔN1-3)tr
LIVBP-like domain
LAOBP-like domain
10-10 10-9 10-8 10-7 10-6 10-5
Zn IC50 (M)

Figure 2

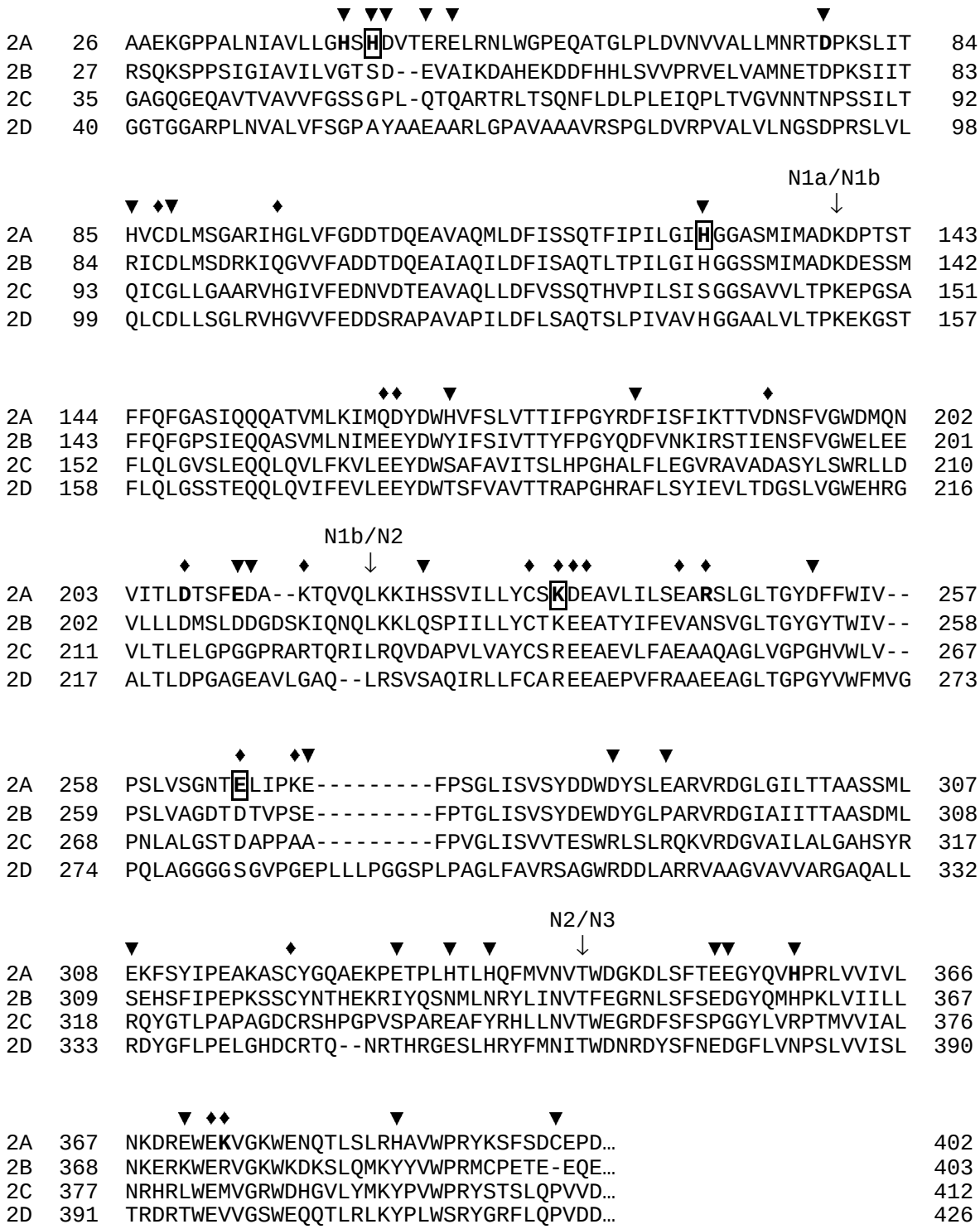
2A 26 AAEKGPPALNIAVLLGHSHDVTERELRNLWGPEQATGLPLDVNVVALLMNRTDPKSLIT 84
2B 27 RSQKSPPSIGIAVILVGTSD--EVAIKDAHEKDDFHHLSVVPRVELVAMNETDPKSIIT 83
2C 35 GAGQGEQAVTVAVVFGSSGPL-QTQARTRLTSQNFLDLPLEIQPLTVGVNNTNPSSILT 92
2D 40 GGTGGARPLNVALVFSGPAYAAEAARLGPAVAAAVRSPGLDVRPVALVLNGSDPRSLVL 98
N1a/N1b
2A 85 HVCDLMSGARIHGLVFGDDTDQEAVAQMLDFISSQTFIPILGIHGGASMIMADKDPTST 143
2B 84 RICDLMSDRKIQGVVFADDTDQEAIAQILDFISAQTLTPILGIHGGSSMIMADKDESSM 142
2C 93 QICGLLGAARVHGIVFEDNVDTEAVAQLLDFVSSQTHVPILSISGGSAVVLTPKEPGSA 151
2D 99 QLCDLLSGLRVHGVVFEDDSRAPAVAPILDFLSAQTSLPIVAVHGGAALVLTPKEKGST 157
2A 144 FFQFGASIQQQATVMLKIMQDYDWHVFSLVTTIFPGYRDFISFIKTTVDNSFVGWDMQN 202
2B 143 FFQFGPSIEQQASVMLNIMEEYDWYIFSIVTTYFPGYQDFVNKIRSTIENSFVGWELEE 201
2C 152 FLQLGVSLEQQLQVLFKVLEEYDWSAFAVITSLHPGHALFLEGVRAVADASYLSWRLLD 210
2D 158 FLQLGSSTEQQLQVIFEVLEEYDWTSFVAVTTRAPGHRAFLSYIEVLTDGSLVGWEHRG 216
N1b/N2
2A 203 VITLDTSFEDA--KTQVQLKKIHSSVILLYCSKDEAVLILSEARSLGLTGYDFFWIV-- 257
2B 202 VLLLDMSLDDGDSKIQNQLKKLQSPIILLYCTKEEATYIFEVANSVGLTGYGYTWIV-- 258
2C 211 VLTLELGPGGPRARTQRILRQVDAPVLVAYCSREEAEVLFAEAAQAGLVGPGHVWLV-- 267
2D 217 ALTLDPGAGEAVLGAQ--LRSVSAQIRLLFCAREEAEPVFRAAEEAGLTGPGYVWFMVG 273
2A 258 PSLVSGNTELIPKE---------FPSGLISVSYDDWDYSLEARVRDGLGILTTAASSML 307
2B 259 PSLVAGDTDTVPSE---------FPTGLISVSYDEWDYGLPARVRDGIAIITTAASDML 308
2C 268 PNLALGSTDAPPAA---------FPVGLISVVTESWRLSLRQKVRDGVAILALGAHSYR 317
2D 274 PQLAGGGGSGVPGEPLLLPGGSPLPAGLFAVRSAGWRDDLARRVAAGVAVVARGAQALL 332
N2/N3
2A 308 EKFSYIPEAKASCYGQAEKPETPLHTLHQFMVNVTWDGKDLSFTEEGYQVHPRLVVIVL 366
2B 309 SEHSFIPEPKSSCYNTHEKRIYQSNMLNRYLINVTFEGRNLSFSEDGYQMHPKLVIILL 367
2C 318 RQYGTLPAPAGDCRSHPGPVSPAREAFYRHLLNVTWEGRDFSFSPGGYLVRPTMVVIAL 376
2D 333 RDYGFLPELGHDCRTQ--NRTHRGESLHRYFMNITWDNRDYSFNEDGFLVNPSLVVISL 390
2A 367 NKDREWEKVGKWENQTLSLRHAVWPRYKSFSDCEPD… 402
2B 368 NKERKWERVGKWKDKSLQMKYYVWPRMCPETE-EQE… 403
2C 377 NRHRLWEMVGRWDHGVLYMKYPVWPRYSTSLQPVVD… 412
2D 391 TRDRTWEVVGSWEQQTLRLKYPLWSRYGRFLQPVDD… 426

Figure 3

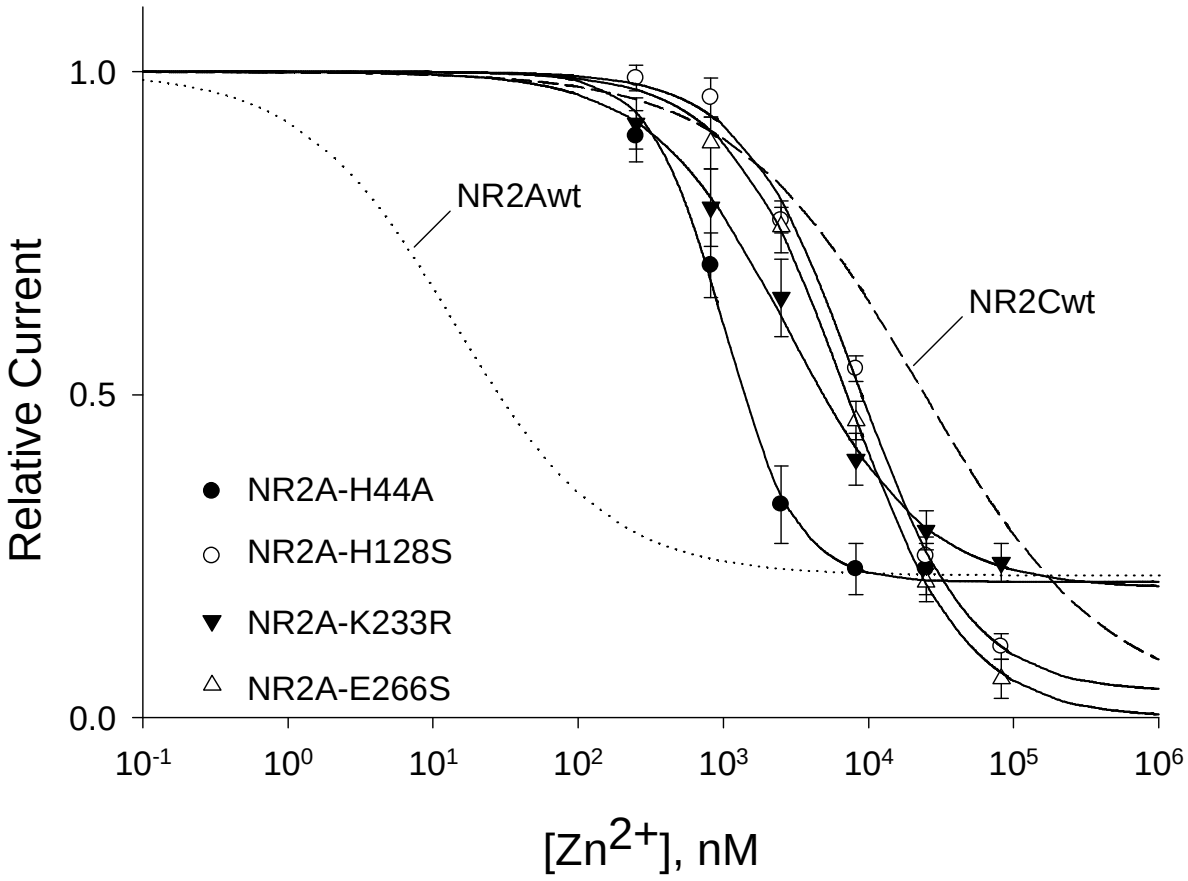
1.0
0.5
0.0
Relative Current
NR2Awt
NR2Cwt
NR2A-H44A
NR2A-H128S
NR2A-K233R
NR2A-E266S
10-1
100
101
102
103
104
105
106
[Zn2+], nM

Figure 4

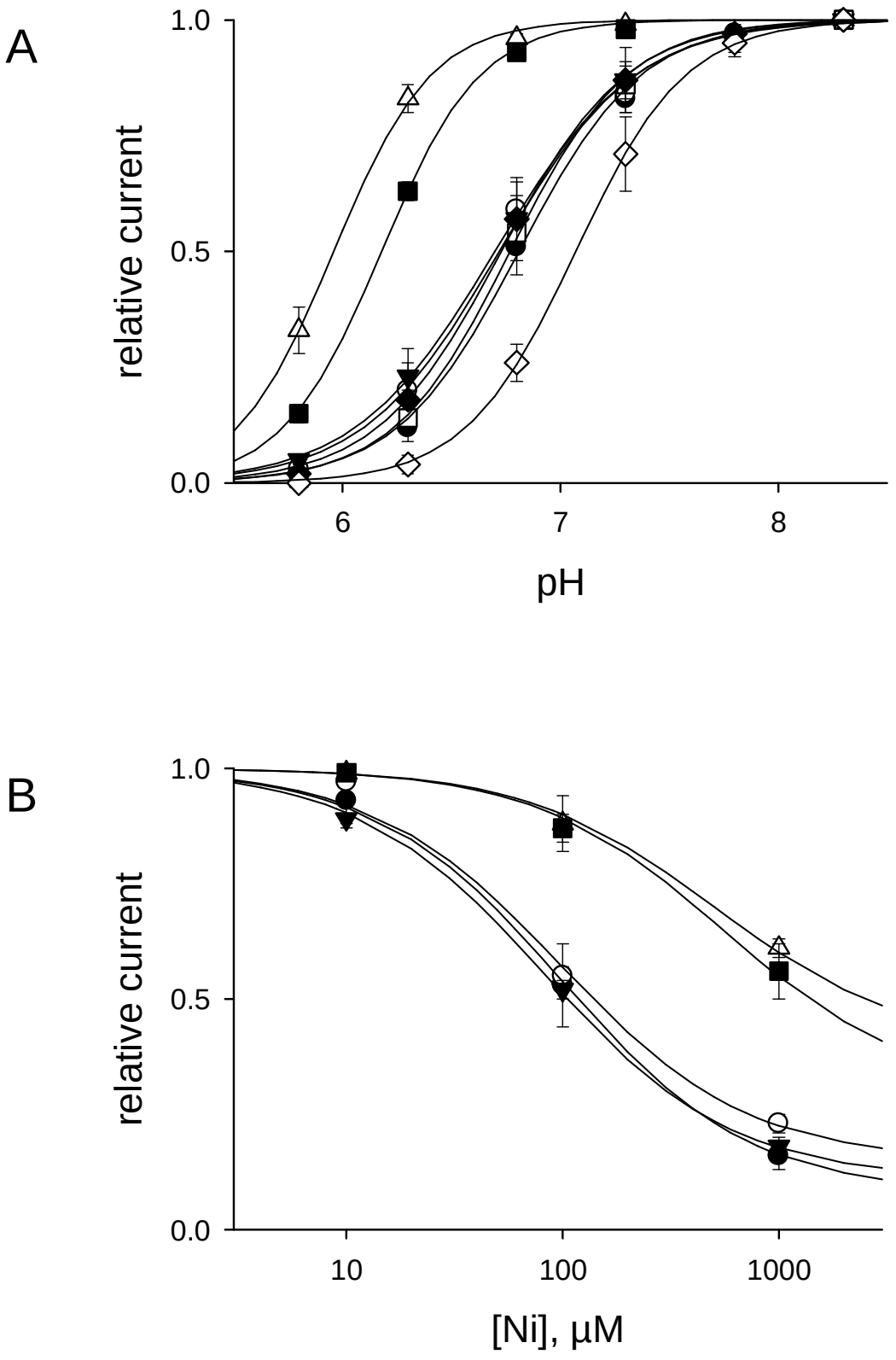
A
1.0
0.5
0.0
relative current
6
7
8
pH
B
1.0
0.5
0.0
relative current
10
100
1000
[Ni], μM

Figure 5